

Manuscript Draft

Manuscript Number: VOLGEO2144R2

Title: Integration of ground-based laser scanner and aerial digital photogrammetry for topographic modelling of Vesuvio volcano.

Article Type: Review Article

Section/Category:

Keywords: Vesuvio

TLS

Aerial Digital Photogrammetry

Models

Integration

Corresponding Author: Dr. Arianna Pesci,

Corresponding Author's Institution: Istituto Nazionale Geofisica Vulcanologia

First Author: Arianna Pesci

Order of Authors: Arianna Pesci, Massimo Fabris, Researcher; Dario Conforti, Researcher; Fabiana Loddo, Researcher; Paolo Baldi, Full Professor; Marco Anzidei, First Researcher

Manuscript Region of Origin:

Abstract: This work deals with the integration of different surveying methodologies for the definition of very accurate Digital Terrain Models (DTM) and/or Digital Surface Models (DSM): in particular, the aerial digital photogrammetry and the terrestrial laser scanning were used to survey the Vesuvio volcano, allowing the total coverage of the internal cone and surroundings (the whole surveyed area was about 3 km x 3 km). The possibility to reach very high precision, especially from the laser scanner data set, allowed a detailed

description of the morphology of the volcano. The comparisons of models obtained in repeated surveys allows a detailed map of residuals providing a dataset that can be used for detailed studies of the morphological evolution. Moreover, the reflectivity information, high correlated to materials properties, allows for the measurement and quantification of some morphological variations in areas where structural discontinuities and displacements are present.

Title:

Integration of ground-based laser scanner and aerial digital photogrammetry for topographic modelling of Vesuvio volcano.

Authors:

Arianna Pesci<sup>1</sup>, Massimo Fabris<sup>2</sup>, Dario Conforti<sup>3</sup>, Fabiana Loddo<sup>1</sup>, Paolo Baldi<sup>2</sup> and Marco Anzidei<sup>4</sup>

Affiliations:

<sup>1</sup>) Istituto Nazionale di Geofisica e Vulcanologia – Sezione di Bologna, via Creti 12, 40128 Bologna, Italy. [pesci@bo.ingv.it](mailto:pesci@bo.ingv.it), [loddo@bo.ingv.it](mailto:loddo@bo.ingv.it)

<sup>2</sup>) Università di Bologna, Dipartimento di Fisica, Settore Geofisica, viale Berti Pichat 8, 40127 Bologna, Italy. [massimo.fabris@unipd.it](mailto:massimo.fabris@unipd.it), [p.baldi@unibo.it](mailto:p.baldi@unibo.it)

<sup>3</sup>) Optech Incorporated, 300 Interchange Way, Vaughan, Ontario, L4K - 5Z8, Canada. [darioc@optech.ca](mailto:darioc@optech.ca)

<sup>4</sup>) Istituto Nazionale di Geofisica e Vulcanologia – CNT, via di Vigna Murata 605, 00139 Roma, Italy. [anzidei@ingv.it](mailto:anzidei@ingv.it)

Corresponding Author (permanent address):

Arianna Pesci

Istituto Nazionale Geofisica Vulcanologia – Sezione di Bologna  
via Donato Creti 12, 40128 Bologna, Italy

Mail: [pesci@bo.ingv.it](mailto:pesci@bo.ingv.it)

Phone: +39 0514151416 / Mobile +39 3339754063

Fax: +39 0514151498

## Abstract

This work deals with the integration of different surveying methodologies for the definition of very accurate Digital Terrain Models (DTM) and/or Digital Surface Models (DSM): in particular, the aerial digital photogrammetry and the terrestrial laser scanning were used to survey the Vesuvio volcano, allowing the total coverage of the internal cone and surroundings (the whole surveyed area was about 3 km x 3 km). The possibility to reach very high precision, especially from the laser scanner data set, allowed a detailed description of the morphology of the volcano. The comparisons of models obtained in repeated surveys allows a detailed map of residuals providing a dataset that can be used for detailed studies of the morphological evolution. Moreover, the reflectivity information, high correlated to materials properties, allows for the measurement and quantification of some morphological variations in areas where structural discontinuities and displacements are present.

## Keywords:

Vesuvio, TLS, Aerial Digital Photogrammetry, Models, Integration

## 1 Introduction

2 Several geophysical processes, involving crustal deformation, can be studied and  
3 monitored by means of the comparison of multitemporal Digital Terrain Models (DTM)  
4 and/or Digital Surface Models (DSM): deformation patterns, displacements, surface  
5 variations, volumes involved in mass movements and other physical features can be  
6 observed and quantified providing useful information on the geomorphological variations  
7 (Achilli et al., 1997; Butler et al., 1998; Kaab and Funk, 1999; Baldi et al., 2000; Kerle,  
8 2002; Mora et al., 2003, van Westen and Lulie Gethaun, 2003; Pesci et al., 2004, Fabris  
9 and Pesci, 2005; Pyle and Elliott, 2006).

10 Several techniques, including GPS kinematic methodology (Beutler et al., 1995), digital  
11 aerial and terrestrial photogrammetry (Kraus, 1998), airborne and terrestrial laser  
12 scanning (Csatho et al., 2005), remote sensors on spaceborne platforms, both optical and  
13 radar stereo option, satellite SAR interferometry (Fraser et al., 2002; Stramondo et al.,  
14 2006), are suitable surveying methods for the acquisition of precise and reliable 3D or  
15 2.5D geo-information. The terrestrial laser scanning (TLS), in particular, measures range  
16 and reflectance characteristics of the observed objects, defining the physical surfaces with  
17 redundant survey points (illuminated elements) and describing the topographic details at  
18 an extremely high accuracy level of few centimetres or better (Ingensand et al., 2003;  
19 Crosilla and Galetto, 2004; Pesci et al. 2006, Pieraccini et al., 2006). Terrestrial Laser  
20 Scanning operates in a similar fashion to a laser range finder, computing the ranges,  
21 measuring the time of flight of a laser pulse with a precision of about 1 cm; moreover, the  
22 laser beam is deflected over a calibrated angular grid providing the automated coverage  
23 of a surface previously defined by the operator. The system computes, for each spot, and  
24 the coordinates of the measured point into the internal reference frame: this is allowed by  
25 the estimate of the baseline and the knowledge of the angle of signal emission. Each laser  
26 pulse illuminates a small area over the target surface and the spot size increases linearly

1 with the range: at 100 meters, for long range new instrument generation, spot size can  
2 reach a diameter of approximately 2 cm increasing to 20 cm at 1000 m distance: the  
3 accuracy of the laser points depends essentially on: distance, to the angle of incidence of  
4 the beam over the surface and quality of the internal telemeter. The large amount of  
5 measured data and the overlapping technique adopted during the scan, allows the user to  
6 obtain higher precisions rates of the laser model in respect to the single point (Geoff,  
7 2005; Boehlr, 2003; Fidera et al., 2004). In general a laser scanner is able to define the  
8 first and the last arrival for each pulse: this allows the user to reduce the effects of  
9 vegetation or other noises above the physical surface (Schulz, 2004). For this reason it  
10 can be adopted for integration on small areas with high resolution surface models usually  
11 obtained via other methods, such as aerial digital photogrammetry. These approaches are  
12 characterized by different accuracy levels, time and costs of execution; airborne surveys  
13 may be adopted in dangerous or inaccessible areas such as steep slopes, landslides,  
14 volcanoes, where ground-based measurements cannot be easily carried out. The quality  
15 of the images, the visibility, the presence of shadows, the acquisition geometry in respect  
16 to the surface orientation (vertical slopes), may degrade the final three-dimensional  
17 restitution of points or prevent the correct stereoscopic coverage.

18 On the other hand, the terrestrial laser scanner is an active instrument limited only by  
19 operational range, which is usually less than 2000 m. A unique feature of terrestrial laser  
20 scanning is that no common station points are required in subsequent surveys because the  
21 results are independent.

22 In this work a complete model of the whole Vesuvio volcano crater and surroundings is  
23 obtained integrating two techniques, which provides highly accurate results over large  
24 areas and overcomes the limits imposed by either method independently.

25 A further consideration about these surveying techniques concerns some  
26 practical/economical aspects. The laser scanner instrument is quite expensive but it can

be rent for short times (few days) at low costs allowing the complete surveying of the interested areas; also the planning of a specific airborne survey is very expensive, but the Italian territory is well covered by stereoscopic images that are often acquired for cartographic purpose by private or public companies (for example, the Istituto Geografico Militare Italiano), so it is possible to acquire the needed frames, for scientific purposes, at low costs.

#### 1. Aerial Photogrammetric survey, processing and model extraction

The active Vesuvio volcano is located in a highly populated area near the city of Napoli (Italy). The volcanic edifice consists of an older stratovolcano, Mt. Somma, whose caldera (5 Km max. diameter) was affected by several collapses, and a recent cone (Vesuvio), which grew within the caldera after the AD 79 “Pompei” eruption (Cioni et al., 1999); the last eruption took place in 1944.

The summit of the Vesuvio cone is at an altitude of 1112 m a.s.l.; the crater rim has a mean diameter of 700 m and the central depression is at a depth of about 300 m respect to the apex of the cone.

On September 9<sup>th</sup> 2004 an aerial photogrammetric survey was performed over Vesuvio volcano acquiring 5 photographs at a mean scale 1:10000; the area included the internal and external slopes of the Vesuvio crater and a large portion of the Somma-Vesuvio caldera. The diapositive film frames (fig.1) were scanned by means of a photogrammetric scanner at 1800 dpi. The obtained ground pixel dimension was about 15 cm.

Following Kraus (1998), it is possible to estimate a theoretical vertical accuracy, strictly depending on the ground pixel dimension, the flight height, the distance between image centres (base of the stereo pairs) and the horizontal accuracy; in this case, taking into account the capability of the correlation algorithms, adopted in the digital analysis, to work at sub-pixel level, the achievable precision is approximately 7 cm.

1  
2 [insert figure 1 – colour web and paper]

3  
4 Seventeen natural Ground Control Points (GCP) were located on the images and  
5 subsequently recognized and measured by means of a GPS campaign performed in  
6 December 2005. At each station, rapid static GPS acquisitions (Hofman et al., 1997) were  
7 executed collecting data at 30 s sampling rate throughout 30 minutes measurement  
8 sessions; observables belonging to three external and permanent stations, located in the  
9 Vesuvian area (Pinguet al., 1998) were used to calculate baselines of the network in post-  
10 processing mode by means of the Bernese 4.2 software (Rothacher et al., 2001).

11 The coordinates of points were computed in to the WGS84 reference frame, and  
12 successively transformed in the cartographic UTM system with sub-centimetre accuracy  
13 for the planimetric components and higher (centimetric level) for the vertical one. The  
14 datum, used to constrain points coordinate over the chosen reference frame, was provided  
15 by the knowledge of permanent station positions. The extraction of a photogrammetric  
16 stereoscopic model was performed using the control point coordinates following the  
17 standard procedures for the inner, relative and absolute orientations, using the Socet Set  
18 software v. 5.3 (SoftCopy Exploitation Tool Set, Bae Systems, 2006). The external  
19 (relative + absolute) orientation results provided rms values for the x, y and z components  
20 of 0.045 m, 0.049 m and 0.032 m, respectively.

21 Following the orientation of the stereoscopic model, a Digital Surface Model (DSM) was  
22 automatically extracted over a 2.5 m x 2.5 m grid size for the whole analyzed area (fig.2),  
23 applying the correlation algorithm based on the “adaptive method” (Baltsavias et al., 2001).  
24 The internal crater and the top edge of volcanic cone were extracted with a 0.5 m x 0.5 m  
25 grid size, increasing the resolution of the model.



1 The definition of a topographic surface, based on points extracted over a regular grid,  
2 implies a relation between the altimetric component and the planimetric ones. For this  
3 reason, it can be used the DSM notation (2.5D), instead of DTM (3D), to emphasize the  
4 not completely independent nature of the third component. The restitution of steep slopes,  
5 or other vertical surfaces, can introduce large modelling errors in the obtained data set due  
6 to the high vertical variation behind two subsequent grid points (Florinsky, 1998; Walker  
7 and Willgoose, 1999).

8 A further consideration concerns the difference between the 'Elevation Model' and  
9 'Terrain Model': the first one represents the entire vertical information of the surveyed  
10 area while the second one is corrected on the physical terrain surface. It is important to  
11 note that only the inner part of the model truly represents the physical terrain surface  
12 (volcanic cone and surroundings), following the editing corrections of the operator.

13  
14 [insert figure 2 – colour web and paper]

15  
16 The Figures Of Merit (FOM) parameter allows for the identification of precision and  
17 validity of the measurement for each extracted point. These integer numerical values range  
18 from 0 to 99; a FOM lower than 33 indicates that the correlation algorithms failed or the  
19 results is questionable, and that an interactive review by an operator is required. Numbers  
20 greater than 32 indicate successful automatic correlation and, in this case, the values are  
21 proportional to the correlation coefficients of the images matching. When the FOM of a  
22 specific post is not acceptable (lower than 33) its elevation is obtained by interpolating or  
23 extrapolating (depending on FOM value) from surrounding data.

24 Few problems were detected during images analysis, except for very limited areas of dark  
25 shadows and extremely steep slopes, where the correlation algorithm failed. In figure 3,  
26 four different maps relating to photogrammetric data processing are shown: the first map

(a) represents a planimetric distribution of FOM values (lower than 33), relating to the model automatically extracted before manual editing, this corresponds approximately 34% of the entire area. Comparing figure 3a to the map of slopes (figure 3b) and to the ortho-photo (figure 3c), the correlation between areas where the automatic extraction is questionable and high slopes, presence of vegetation and poor illumination conditions exist (east part of the internal crater) are evidenced. The manual review and editing was performed over these zones, that is approximately 30% of the total area, allowing the definition of the final reference DSM: the last map (d) included in figure 3, shows residuals between the previous DSM (extracted by a totally automated procedure) and the reference one. Also in this case it is evident that corrections were mainly applied over zones characterized by low FOM, but the area which really needed manual editing was reduced in respect to the indications provided in the FOM map (a), as directly checked by the operator in a stereoscopic view: on the other hand the interpolation tools, introduced by the automatic procedures, in some cases are quite effective and efficient.

The final photogrammetric model, given in the WGS84 system, and relative to the September 2004 survey, was considered as the reference model due to the measured GCP distributed both around the internal cone and in the external areas.

[insert figure 3 – colour web and paper]

## 2. Terrestrial Laser Scanner survey

In May 2005, a Terrestrial Laser Scanner survey was conducted over the Vesuvio crater by means of the ILRIS-3D instrument (Optech inc., 2005). Twenty scans were acquired in just a few hours (fig.4), covering the entire crater from 4 different station points. The ILRIS positions were measured by GPS observations performed to register the final point cloud into the external WGS84 reference frame; a further stationing point was considered

(black dot in fig.4) but it was impossible to access the area due to instabilities and potential hazards. These conditions prevented the optimization of the scan and complete definition of the model because a critical requirement of the method is to measure the surface as normally and uniformly as possible with while avoiding a stretched beam footprint. Each scan was characterized by a high number of shots (up to 2 millions) and a mean spot spacing value of the same order of spot dimension, ranging from 6 to 12 cm, depending on the range.

[insert figure 4 – colour web and paper]

All scans were aligned, pair to pair, starting from a preliminary rough registration, manually detecting homologous points over images, estimating roto-translational parameters and applying ICP (Interactive Closest Points) algorithms, available in the Polyworks software (Innovmetric inc.) to improve the registration. The strategy was to minimize the distance between points from the first frame and the tangent planes at intersected points in the second one, thereby decreasing the mean and standard deviation of residual distribution from centimetre to millimetre values: this strategy is appropriate because the two surface distances are minimized, and their curvatures are locally matched (Bergevin et. al, 1996). The analysis of residuals between scans, provided a mean standard deviation of about 8 cm, taking into account all available data points.

The last step was the transformation of the point cloud from the local system to the WGS84 reference frame, was to impose GPS coordinates to the station points by means of a roto-translation transformation.

Overlaps were reduced to decrease redundant points, avoiding processing problems due to memory overflow; the resulting cleaned point cloud was finally meshed to provide a triangulated model (5 cm mean length). This choice allowed a good surface description,

1 reducing data storage as much as possible and providing suitable digital representation of  
2 the surface, volume evaluation and morphometric applications. The model extracted is  
3 characterized by a high definition; this fact confirms the scanner efficiency at ranges of  
4 over 600 meters or more, and also proves high performans characteristics even on low  
5 reflectance surfaces. There were very few problem areas due to data gaps; this gaps are  
6 essentially due to occlusion or inaccessibility limitation and the position of station points  
7 with respect to the surveyed area.

8 For instance, the upper rim as a lower precision rating due to the spot spreading caused by  
9 the small angle between the incident ray and the surface (but the laser sensor associate the  
10 computed distance to the theoretical spot centre). The beam footprint, in fact, rapidly  
11 increases providing a worse point measurement: on the SW part of the cone the beam  
12 footprint reached length values of the order of 1 m for 600-700 m ranges.

13 Moreover, the tangent beam geometry acquisition causes longer shadows enlarging the  
14 data gap while, a normal incident angle causes a reduced data loss effect.

15 Figure 5 shows the areas where triangles (belong to the triangulated model) significantly  
16 differs from the topography (red lines); the lower resolution in the crown is evidenced by  
17 the dashed yellow lines.

18  
19 [insert figure 5 – colour web and paper]

### 20 21 3. Data integration

22 As stated both aerial digital photogrammetry and terrestrial laser scanning are very  
23 efficient tool for surfaces modelling applications, but the quality of the individual data set  
24 is quite different: the results, given at variable scales and resolutions, are degraded by  
25 different sources of errors. In this case, the presence of very corrugated surfaces and steep  
26 slopes required ultra-high images quality but it was very difficult to define accurate

models over vertical surfaces and poor illumination. Moreover, some data gaps did occur during the surveying of Vesuvio when the terrestrial laser scanner was being used because of the impossibility to access the northern part of the top of the cone (this is a no-flight zone without an expert professional guide). For these reasons the integration of these two data set is extremely useful. Figure 6 shows two clear examples of the limits of modelling by digital photogrammetry and laser scanning. Two areas inside A and B boxes, indicated in figure 5, are shown by a front view.

The first sample (A) describes excellent integration of the two data set. Any gaps in the terrain laser data can be subsequently filled using the information provided by the digital airborne photogrammetry that appears clearly complete. The second example (B) shows great differences between the two data set: the high verticality and the presence of shadows, degraded the photogrammetric images and consequently the possibility of a correct model extraction: in this case only the terrain laser data is used.

[insert figure 6 – colour web and paper]

Two cross sections were obtained from the intersection of the crater and a North-South vertical plane: points belonging to laser and photogrammetric models were graphicated in red and blue respectively and two zones in the left and right part of the plane are zoomed. A further example of the different quality of results obtained by the two methods is shown in figure 9, which relates to a cross section of the crater area obtained from the intersection of the crater and a vertical plane  $0^\circ$  oriented (EW direction). Points belonging to laser and photogrammetric models were graphicated in red and blue respectively and two zones in the left and right part of the plane are zoomed.

On the left is an excellent integration of the two data set and the laser data gap (which will be subsequent filled in using the information provided by the digital

1 photogrammetry): the reader should notice that the laser points belonging to the crossing  
2 plane were drawn to highlight data gaps.

3 On the right part the high verticality and the presence of shadows degraded the  
4 photogrammetric restitution. Here the integration was not useful in improving the final  
5 model: it should be noted that the photogrammetric model of the steep slope is  
6 characterized by a lower accuracy respect to the ground-based laser model.

7 In the figure are shown two statistical distribution of residuals (point to plane minimum  
8 distance) computed between cross section data sets in the left and right part of the plane  
9 which represent the SW and NE crater domain. The first is zero-centred and characterized  
10 by 0.20 m standard deviation, while the second shows a systematic effect and a larger  
11 deviation of about 2 m.

12  
13 [insert figure 7 – colour web and paper]

14  
15 These evidences make it necessary an integration of the two techniques; it was performed  
16 thereby overcoming the limits imposed by each technique to obtain a unique and complete  
17 model from the two data set.

18 It is important to note that despite dramatic events which drastically change the entire  
19 morphology of the volcano crater and surroundings, the expected variations are in general  
20 related to small percentage of the area. Using the same procedure described above for  
21 scans registration (Polyworks software) the two models were aligned and residuals were  
22 computed (fig.8). First, the operator checked to see if the areas with the greatest  
23 discrepancies coincide with the ones containing a data gap or poor vertical resolution (for  
24 example the steepest slopes observed by air platform). Subsequently, these areas were  
25 excluded from the computation and a new alignment was performed: in this way the  
26 models were correctly registered in the same reference frame. Finally, the complete

1 definition of an error map was performed, computing residual vectors that minimize the  
2 point to plane distances of one model to the other.

3  
4 [insert figure 8 – colour web and paper]

5  
6 The distribution of the three components (North, East and Up) of the residual vectors were  
7 analyzed providing negligible values for the mean and standard deviation lower than 20  
8 cm (fig.9).

9  
10 [insert figure 9 – colour web and paper]

11  
12 Finally, the photogrammetric data coinciding to laser data gaps inside the crater and over  
13 the crown (oriented in the same reference system) were used to patch and fill the cloud of  
14 points and a new and complete internal model was computed with a limited resolution  
15 degradation factor. The integration was obtained by taking into account the different  
16 precisions of data in the internal crater. In particular, these internal zones were primarily  
17 modelled using laser data and filling all the data gaps with the photogrammetric one.

18 This procedure was performed in a simple fashion: the two models were rigorously aligned  
19 providing rototranslation matrices for a correct registration.; photogrammetric coordinates  
20 of extracted points were selected to cover laser scanner data gap in the internal part of the  
21 cone providing the necessary information for a new and complete model reconstruction.

22 In general the terrestrial laser scanner data set is truly denser and more accurate in respect  
23 the others: for this reason the photogrammetric data was used principally to fill in data  
24 gaps in laser clouds.

25 Despite the fact that the laser cloud of points were very dense and the original triangulated  
26 model was obtained with mean size of 5 cm, the internal crater was defined at

1 approximately a 20-30 cm resolution level, to avoid memory data flow in the next  
2 processing, increasing to 0.5 m when the only data available was photogrammetric.  
3 The final triangulated model obtained by the integration, was characterized by a mean 20-  
4 30 cm internal resolution, about 50 cm on the cone edge and 2.5 m for the external part of  
5 the Vesuvio (fig.10).

6  
7 [insert figure 10 – colour web and paper]  
8

#### 9 4. Analysis

10 The last eruption of Vesuvio occurred in 1944 and its actual state of activity is quiescent,  
11 with presence of fumaroles and low local seismicity inferred to gravitational loading of  
12 the volcanic edifice (De Natale et al., 2000). Following the eruptive phases till the end of  
13 explosions (March 29<sup>th</sup>, 1944) the crater experienced numerous settlements essentially  
14 due to landslides which changed its morphology.

15 Investigating surface deformations, many authors reported relevant values of a  
16 progressive subsidence of the cone, with rates reaching 0.05-0.06 m/y, confirmed by  
17 levelling data analysis and differential SAR interferometry (Pingue et al., 2000; Lanari et  
18 al., 2002): in particular, these measures refer to the Vesuvio cone (Gran Cono) while the  
19 volcanic edifice seems to be very stable throughout years since 1992.

20 Due to the extremely high resolution of the model, obtained by terrestrial laser scanning  
21 and photogrammetry integration, extending few kilometres around the cone, it is possible  
22 to extract much geometrical and geomorphological information. At first, the analysis  
23 started creating several cross sections. These lines were obtained intersecting vertical  
24 planes to the crater model, following an angular sequence of 10° starting from the WE  
25 horizontal direction. In the figure 11 two interesting sections (plotted over the 2D plane)  
26 are shown related to 0° and 30° angles. The crater is clearly divided into two zones



1 characterized by different slopes: the main inclination of the NE portion is about 75°  
2 dipping while the SW part is often lower than 40°. This is also apparent by the curvature  
3 of the upper cone pipe, which shows two different values in the NE and SW zones: the  
4 first one is fitted with a circle of about 195 m radius, while for the second one, about 340  
5 m radius is needed (fig.11).

6  
7 [insert figure 11 – colour web and paper]

8  
9 Looking at the two zones of peculiar topographic discontinuity, coinciding to disrupted  
10 areas where relevant landslides may be recognized, another vertical plane was fitted and a  
11 new cross section was created. The obtained trend shows a mean inclination of 30° and  
12 40° on the two sides of the section (fig.11) which provides evidence of a lower than mean  
13 slope of the crater; this plain clearly divides the caldera in two parts with quite different  
14 morphological aspects.

15 This section is a specific line corresponding to the presence of high erosion and debris  
16 accumulation; the fractured zones, which geometry is well defined by the model,  
17 observed by both optical and reflectance images (the second is a data set coloured by the  
18 intensity of the signal energy) shows the same stratification passing through the two sides  
19 of the crater, suggesting a strong dislocation effect (fig. 12).

20  
21 [insert figure 12 – colour web and paper]

22  
23 The high correlation between materials and reflectivity enables the definition of the  
24 stratigraphy and to allows the quantification of the dislocation: in particular, a mean step  
25 value of about 1.5 m was observed throughout the rupture surface, showing a relative  
26 lowering of the NE portion. This measurement and the geometrical and morphological

1 identification of a plane that clearly separates the crater in two different parts, seems to be  
2 in agreement with Bianco et al. (1998) thus reinforcing the hypothesis of a NW-SE  
3 trending fault system.

4 A further inspection of the point clouds was performed over the opposite site of the crater  
5 area where the second main landslide lies (NW). In this case, unfortunately the highly  
6 disrupted surface didn't allow for the correlation between morphology and signal  
7 intensity to detect steps. Despite the landslides located in the two main morphological  
8 discontinuities zones and the measured displacement along the SW breaking, these  
9 indicators are necessary but not sufficient to prove the presence of a fault plane: the  
10 observed variation could also depend on local gravitational effects, acting over a  
11 fractured rock unit.

12 These quantitative and qualitative inspections achievable from laser scanning can support  
13 the volcanological community in sampling rocks and producing very accurate  
14 stratigraphy of the crater in order to better define the genesis of the volcano. The first  
15 geomorphological map of Vesuvio at a 1:10000 scale was recently presented (Ventura et  
16 al., 2005), including volcanic and epivolcanic landforms. The radiometric information  
17 provided by terrestrial laser scanner, associated with the high resolution of the model,  
18 allows for the identification of different layers by means of the correlation between  
19 physical and geological details (Akiyama and Sasaki, 2002), extracting information from  
20 geological elements belonging to the caldera. Scoria are well recognized in the upper part  
21 of the scar of the volcano vent and irregular successions of compact lava strata are also  
22 evident (fig.14).

23 Moreover, the high definition and dense coverage of the model over the entire crater and  
24 over areas adjacent to debris accumulations suggest that monitoring can be easily  
25 obtained by means of repeated and fast (few hours) laser scanner surveys from which  
26 relative volume variations can be computed.

[insert figure 13 – colour web and paper]

## 5. The last survey

In October 2006 the Istituto Nazionale di Geofisica e Vulcanologia (INGV), in the context of a national exercitation organized by the Dipartimento della Protezione Civile (DPC), executed the second laser survey of the whole crater using the advanced scanner ILRIS3D-ER (Enhanced Range). As the name denotes, the ILRIS3D-ER has a capacity to extend it's traditional range by up to 40% as compared to the previous ILRIS3D version. The preliminary fast processing allowed for the direct recognition of zones characterized by higher intensities due to a collapse of a portion of some slopes. The alignment and comparison of point clouds (2006-2005) shows high variations over a large portion of the NE slope and a volume variation of about 6850 m<sup>3</sup> was computed.

[insert figure 14 – colour web and paper]

This result was obtained in a very short time (within a few hours after the end of the measurement campaign) from scans comparisons which suggest that this kind of surveying may lead to an efficient control system. It can also be utilized during times of emergency, and to significantly improve the description of the landscape in areas which can be difficult to access in terms of precision immediate execution..

## 6. Conclusions

In this work the global model of the Vesuvio volcano was obtained by integrating data which belongs to two different surveying methodologies. The terrestrial laser scanner enabled the generation of a very accurate model of the internal crater, aligning 20 scans

1 acquired from 4 stationing points, at approximately a 5 cm resolution level that was  
2 successively reduced to about 30 cm for computational proposal. The orientation was  
3 performed using WGS84 coordinate values of the station points measured by means of  
4 GPS.

5 The aerial digital photogrammetry led to a 50 cm resolution model of the same area (the  
6 internal cone) and to a 2.5 m resolution model for the external zones, automatically  
7 processing 5 images and manually correcting limited extracted points over areas where  
8 the correlation FOM parameter was lower than 33.

9 The integration of these two technologies provided a very dense and complete model of  
10 the whole crater and extensive morphological information of the surrounding area  
11 (approximately 9 square kilometres), and the distribution of residuals between  
12 photogrammetric and laser data, excluding zones characterized by significant errors,  
13 shows a standard deviation of about 20 cm.

14 Moreover, the work was completed which produced a model of a large portion of  
15 territory around Napoli: a DTM, obtained digitizing contour lines of a map with mean  
16 size of 20 m, was used to enlarge the studied area (it was aligned following the same  
17 procedures described above by means of Polyworks software, thus minimizing residuals  
18 between points over the common areas). The complex morphology of this volcanic area  
19 is well described by means of terrestrial laser scanning due to the high accuracy, the  
20 long range and a very dense point acquisition over various surfaces (i. e. a million  
21 points for each scan). Also the terrestrial laser scanner equipments (commercial) and  
22 processing software, the great availability of stereoscopic metric images over the Italian  
23 territory and the powerful automatic processing systems, make it possible to obtain  
24 detailed surface models in a very short period of time.

1        Acknowledgment:

2        The authors are grateful to Andrea Faccioli, Marco Bacciocchi and CODEVINTEC  
3        Italiana for his gracious use the ILRIS3D scanner and for the precious assistance  
4        during data processing; a special thank to AVIORIPRESE and to Livio Pinto, Daniele  
5        Passoni and Alessandra Borghi who provided high quality photogrammetric images; we  
6        are also thankful to Folco Pingue for his kind support in planning and executing surveys  
7        and to Nicola Cenni, Prospero De Martino and Vincenzo Sepe for GPS data collection.  
8        Finally, thanks is to Guido Ventura who provided a precious bibliography for  
9        geological studies.

References:

- Achilli, V., Baldi, P., Baratin, L., Bonini, C., Ercolani, E., Gandolfi, S., Anzidei, M., Riguzzi, F., 1997. Digital photogrammetric survey on the island of Vulcano. *Acta Vulcanologica* 9 (2), 1-5.
- Akiyama, H. and Sasaki, S., 2002. Effects of rock coating on reflectance spectra of rock samples. *Solar System Remote Sensing Symposium*, Pittsburgh, Pennsylvania, September 20-21, 2002.
- Baldi, P., Bonvalot, S., Briole, P., Marsella, M., 2000. Digital photogrammetry and kinematic GPS for monitoring volcanic areas. *Geophysics Journal International* 142 (3), 801-811.
- Baltsavias E.P., Favey E., Bauder A., Bosch H., Pateraki M., 2001. Digital surface modelling by airborne laser scanning and digital photogrammetry for glacier monitoring. *Photogrammetric Record* 17 (98), 243-273.
- Bergevin R., Soucy, M., Gagnon, H., Laurendeau, D., 1996. Towards a general multi-view registration technique. *IEEE transaction on patterns analysis and machine intelligence* 18, 540-547.
- Beutler, G., Hein, G.W., Melbourne, W.G., Seeber, G., 1995. GPS trends in precise terrestrial, airborne, and spaceborn applications, *Int. Assoc. Geod. Symp.* 115, 275-338.
- Bianco, F., Castellano, M., Milano, G., Ventura, G., Vilaro, G., 1998. The Somma-Vesuvius stress field induced by regional tectonics: evidenced from seismological and mesostructural data. *Journal of Volcanology and Geothermal Research* 82, 199–218.
- Boehler, W., Bordas Vicent, M., Marbs, A., 2003. Investigating laser scanner accuracy. *XIXth CIPA SYMPOSIUM*, Antalya, Turkey, 30 Sep. - 4 Oct. 2003.

1 Butler, J.B., Lane, S.N., Chandler, J.H., 1998. Assessment of DEM quality for  
2 characterizing surface roughness using close range digital photogrammetry.  
3 Photogrammetric Record 16 (92), 271-291.

4 Cioni, R., Santacroce, R., Sbrana, A., 1999. Pyroclastic deposits as a guide for  
5 reconstructing the multi-stage evolution of the Somma-Vesuvio Caldera. Bulletin of  
6 Volcanology 60, 207-222.

7 Crosilla, F. and Galetto, R., 2004. La tecnica del laser scanning. Teoria ed  
8 Applicazioni. International Centre for mechanical sciences, Collana di Geodesia e  
9 Cartografia pp.184.

10 Csatho, B., Schenk, T., Krabill, W., Wilson, T., Lyons, W., McKenzie, G., Hallam,  
11 C., Manizade, S., Paulsen, T., 2005. Airborne Laser Scanning for High-Resolution  
12 Mapping of Antarctica, EOS 86 (25), 21 June 2005.

13 De Natale, G., Petrazzuoli, S. M., Troise, C., Pingue, F., Capuano, P., 2000. Internal  
14 stress field at Mount Vesuvius: a model for background seismicity at a central  
15 volcano. Journal of Geophysical Research 105 (16), 207-214.

16 Florinsky, IV., 1998. Combined analysis of digital terrain models and remotely sensed  
17 data in landscape investigations. Progress in Physical Geography 22 (1), 33-60.

18 Geoff, J., 2005. Understanding Laser Scanner terminology. Professional Surveyor  
19 Magazine, 22 – 28, February 2005.

20 Hofman-Wellenhof, B., Lichtenegger, H., Collins, J., 1997. GPS Theory and Practice,  
21 edited by Springer Verlag Wien, New York, 214-258.

22 Lanari, R., De Natale, G., Berardino, P., Sansosti, E., Ricciardi, G.P., Borgstrom, S.,  
23 Capuano, P., Pingue, F., Troise, C., 2002. Evidence for a peculiar style of ground  
24 deformation inferred at Vesuvius volcano. Geophysical Research Letters 29 (9) 1010-  
25 1029.

1 Fabris, M. and Pesci, A., 2005. Automated DEM extraction in digital aerial  
2 photogrammetry: precisions and validation for mass movement monitoring. *Annals of*  
3 *Geophysics* 48, 973-988.

4 Fraser, C. S., Baltsavias, E., Gruen, A., 2002. Processing of Ikonos imagery for  
5 submetre 3D positioning and building extraction. *ISPRS Journal of Photogrammetry*  
6 *and Remote Sensing* 56, 177-194.

7 Fidera, A., Chapman, M.A., Hong, J., 2004. Terrestrial Lidar for industrial metrology  
8 applications: modeling, enhancement and reconstruction. XXth ISPRS congress, 12-  
9 23 July 2004, Istanbul, Turkey.

10 Ingesand, H., Ryf, A., Schulz, T., 2003. Performances and experiences in terrestrial  
11 scanning. *Proc. Optical 3D Measurement Techniques*, 22-25 September, Zurich,  
12 Switzerland, pp. 236-244.

13 Kaab, A. and Funk, A., 1999. Modelling mass balance using photogrammetric and  
14 geophysical data: a pilot study at Griesgletscher, Swiss Alps. *Journal of Glaciology*,  
15 45 (151), 575-583.

16 Kerle, N., 2002. Volume estimation of the 1998 flank collapse at Casita volcano,  
17 Nicaragua - a comparison of photogrammetric and conventional techniques. *Earth*  
18 *Surf Process Landforms* 27, 759-771.

19 Kraus, K., 1998. *Fotogrammetria* (Levrotto & Bella, Torino), pp. 445-496.

20 Lanari, R., De Natale, G., Berardino, P., Sansosti, E., Riciardi, G.P., Borgstrom, S.,  
21 Captano, P., Pingue, F., Troise, C., 2002. Evidence for a peculiar style of ground  
22 deformation inferred at Vesuvius volcano. *Geophysical Research Letters* 29, 1025-  
23 1029.

24 Bae Systems, 2006. *SOCET SET User's Manual*, San Diego.

25 Mora, P., Baldi, P., Casula, G., Fabris, M., Ghirotti, M., Mazzini, E., Pesci, A., 2003.  
26 *Global Positioning Systems and digital photogrammetry for the monitoring of mass*  
27



movements: application to the Ca' di Malta landslide (northern Apennines, Italy).  
 Engineering Geology 68, 103-121.

Optech, 2005. Optech announces next-generation ILRIS-3D laser scanner,  
[www.optech.ca/pdf/press/press\\_ilris\\_nextgen.pdf](http://www.optech.ca/pdf/press/press_ilris_nextgen.pdf) (last access: June 2005).

Pesci, A., Baldi, P., Bedin, A., Casula, G., Cenni, N., Fabris, M., Loddo, F., Mora, P.,  
 Bacchetti, M., 2004. Digital elevation models for landslide evolution monitoring:  
 application on two areas located in the Reno River Valley (Italy). Annals of  
 Geophysics 47, 1339-1353.

Pieraccini, M., Noferini, L., Mecatti, D., Macaluso, G., Atzeni, C., Teza, G., Galgaro,  
 A., Zaltron, N., 2006. Radar interferometry and laser scanning for monitoring the  
 stability of an alpine urban site. IEEE Transactions on Geoscience and Remote  
 Sensing 44 (9), 2335-2342.

Pingue, F., Troise, C., De Luca, G., Grassi, V., Scarpa, R., 1998. Geodetic monitoring  
 of Mt. Vesuvius, Italy, based on EDM and GPS surveys. Journal of Volcanology and  
 Geothermal Research 82, 151-160.

Pingue, F., Berrino, G., Captano, P., Obrizzo, F., De Natale, G., Esposito, T., Serio,  
 C., Tammaro, U., De Luca, G., Scarpa, R., Troise, C., Corrado, G., 2000. Ground  
 deformation and gravimetric monitoring at Somma-Vesuvius and Campanian volcanic  
 areas (Italy). Physics and Chemistry of the Earth 25, 9-11, 747-754.

Pyle, D.M., Elliott, J.R., 2006. Quantitative morphology, recent evolution and future  
 activity of the Kameni islands volcano, Santorini, Greece, Geosphere 2 (5), 253-268.

Rothacher, M., Beutler, G., Bock, H., Brockmann, E., Dach, R., Fridez, P., Gurtner,  
 W., Hugentobler, U., Ineichen, D., Johnson, J., Meindl, M., Mervart, L., Schaer, S.,  
 Springer, T., Weber, R., 2001. Bernese Gps Software Version 4.2, Edited By U.  
 Hugentobler, S. Schaer And P. Fridez (On Line:  
[Http://www.civil.uwaterloo.ca/hydrology/Bernese/Bernese\\_4.2\\_Guide.Pdf](http://www.civil.uwaterloo.ca/hydrology/Bernese/Bernese_4.2_Guide.Pdf)).

1 Schulz, T. and Ingensand, M., 2004. Influencing variables, precision and accuracy of  
2 terrestrial laser scanners. INGENO 2004 and FIG Regional Central and Eastern  
3 European Conference of Engineering Surveying, Bratislava, Slovakia, November 11-  
4 13, 2004.

5 Ventura, G., Vilaro, G., Bronzino, G., Gabriele, G., Nappi, R., Terranova, C.,  
6 2005. Geomorphological map of the Somma-Vesuvius volcanic complex (Italy).  
7 Journal of Maps 30-37.

8 Walker, J.P., Willgoose, G.R., 1999. On the effect of digital elevation model accuracy  
9 on hydrology and geomorphology. Water Resources Research 35 (7), 2259-2268.

10 van Westen, C. J. and Lulie Getahun, F., 2003. Analyzing the evolution of the Tessina  
11 landslide using aerial photographs and digital elevation models. Geomorphology 54,  
12 77-89.

Figure captions:

Fig.1 – Photogrammetric frames provided by “Nuova AVIORIPRESE srl”. Despite the poor illumination of about a 20% of the crater, tones were not dark enough to prevent stereoscopic analysis.

Fig.2 – The photogrammetric model derived by extracted DSM: the grid size in the internal part is 0.5 m while in the external part is 2.5 m. Dots indicate ground control points used for the orientation of the images.

Fig.3 – Four maps showing: a) the planimetric distribution of FOM (integer numbers) lower than 33; b) slopes; c) orthophoto and d) vertical residuals between edited model and the automatically extracted one.

Fig.4 – Prospective Vesuvio view: 20 scans coverage. The black circle indicates a planned but not used station point cause access forbidden. ‘1’ and ‘2’ stationing points differs of few metres only: the instrument was moved to overcome some obstacles which could cause data loss.

Fig.5 – High definition model of Vesuvio crater from TLS data: red polygons and yellow lines indicate data gap and points acquired by a low incident angle geometry, preventing respectively correct and precise morphology description. The dashed blue line represent the 0° cross section used for the next discussion. The figure shows the graphical interface of the Polyworks software, used for model creation and previous alignment procedures.

Fig.6 – Aerial digital photogrammetry (yellow) vs Terrestrial Laser Scanning (grey). On the left: the dashed line contains the same physical surveyed areas, revealing data gap in terrestrial laser application. On the right: the photogrammetric model failed over vertical and steep walls.

Fig.7 – A cross-section of the laser (red line) and photogrammetry (blue line) data over the plane (2D visualization). A) the lines lie on the left side of the intersecting plane and

height residuals are well represented by a normal distribution with null mean and 0.2 m of standard deviation. B) the bad modelled vertical slopes by means of digital photogrammetry cause a systematic effect: residuals distribution is affected by a mean of about 2 m.

Fig.8 – Residuals from the alignment of TLS and Photogrammetric models: the orientation is chosen to better evidence discrepancies.

Fig.9 – Residuals distribution for each Cartesian component.

Fig.10 – a) A rough model of Napoli and surroundings over a 20 m x 20 m grid, extracted by the cartographic maps available at the Osservatorio Vesuviano (INGV); b) the area involved by photogrammetric survey; c) Vesuvio cone at 2.5 m resolution and the crater zone at 0.5 m; d) the final and complete internal model obtained by TLS and aerial digital photogrammetry integration: the resolution is mainly the same one of laser point cloud, ranging from 0.3 m to 0.5 m.

Fig.11 – Geometrical considerations: circles are fitted using data over an horizontal plane at the top of the crater and all the cross sections (red and yellow lines) were created and analyzed, showing different slopes over the SW and NE sides.

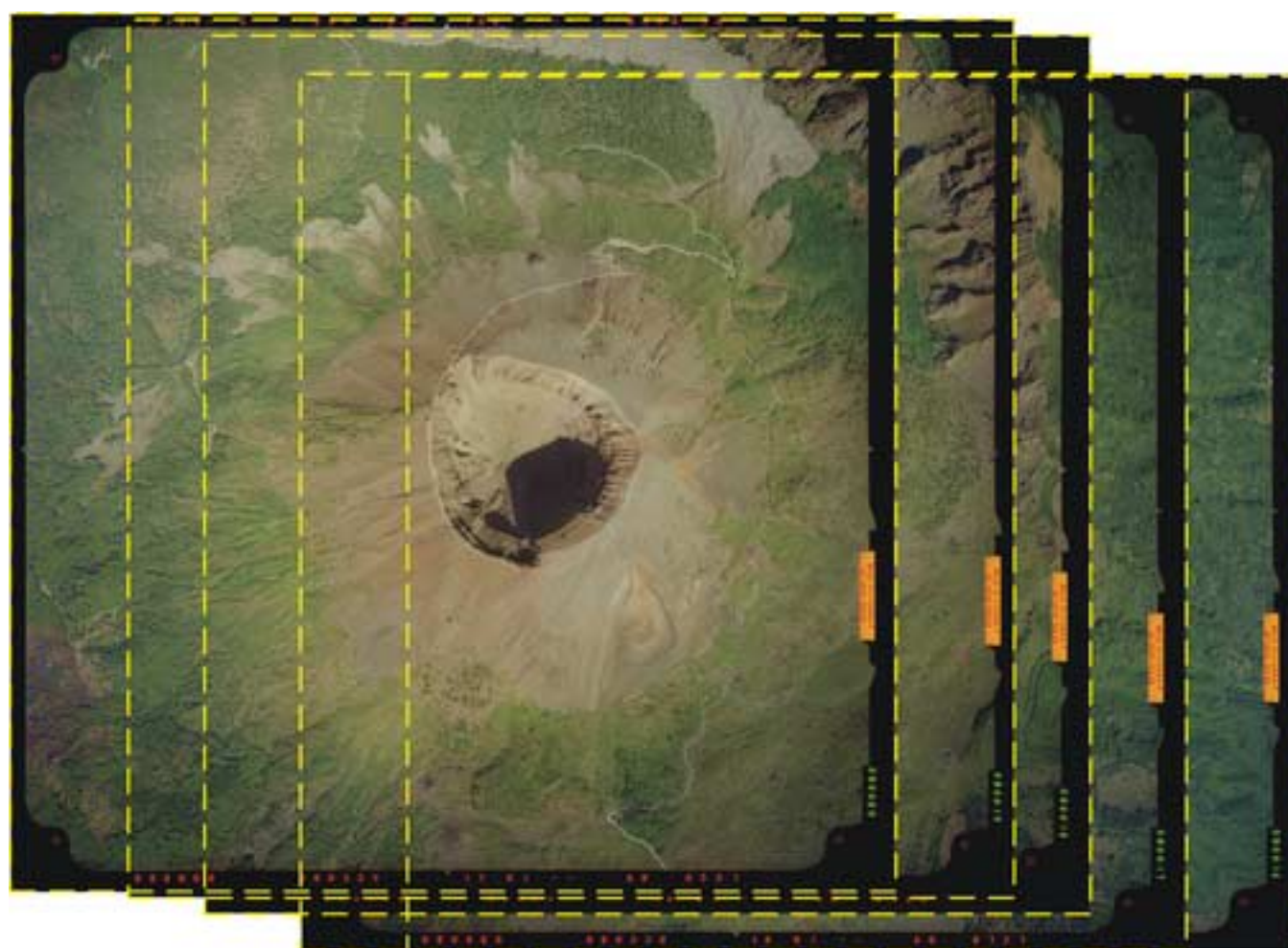
Fig.12 – The point cloud of the SE part of the crater. The fractured zone inside the red box shows high correlation between stratigraphy and reflectivity. In particular, a step of about 1 m is measured, showing a relative lowering of the NE portion respect to the SW one. The yellow line indicates the limits of the two part of the cone with different geometric shape.

Fig.13 – Stratigraphy and correlation between materials and reflectivity response.

Fig.14 – The variations observed in the SE slope of the crater (red box on the left).

Residuals are the point to surface distances computed between aligned 2006 and 2005 scans.

Figure1  
[Click here to download high resolution image](#)



Photogrammetric frames

Figure2  
[Click here to download high resolution image](#)

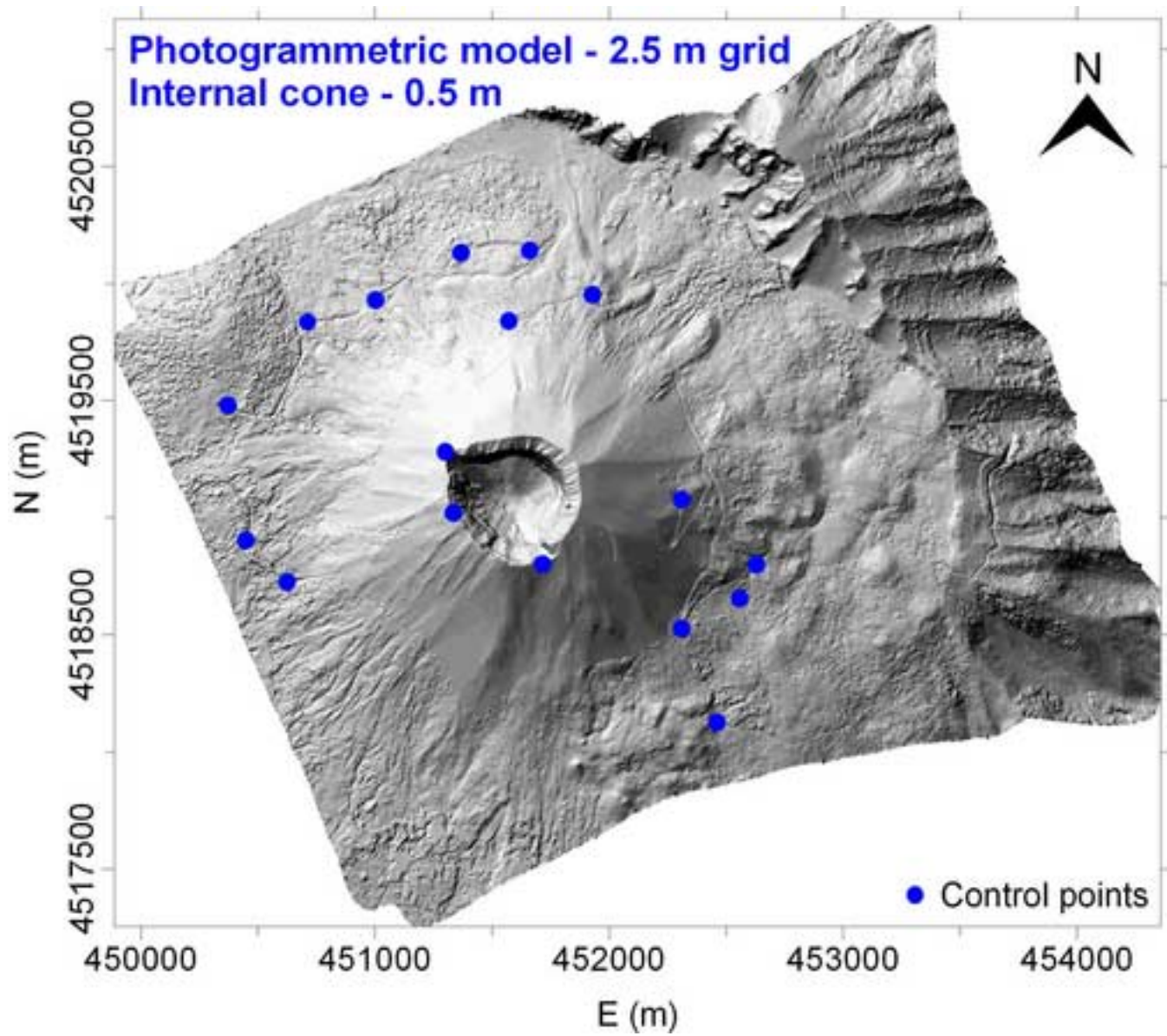




Figure3  
[Click here to download high resolution image](#)

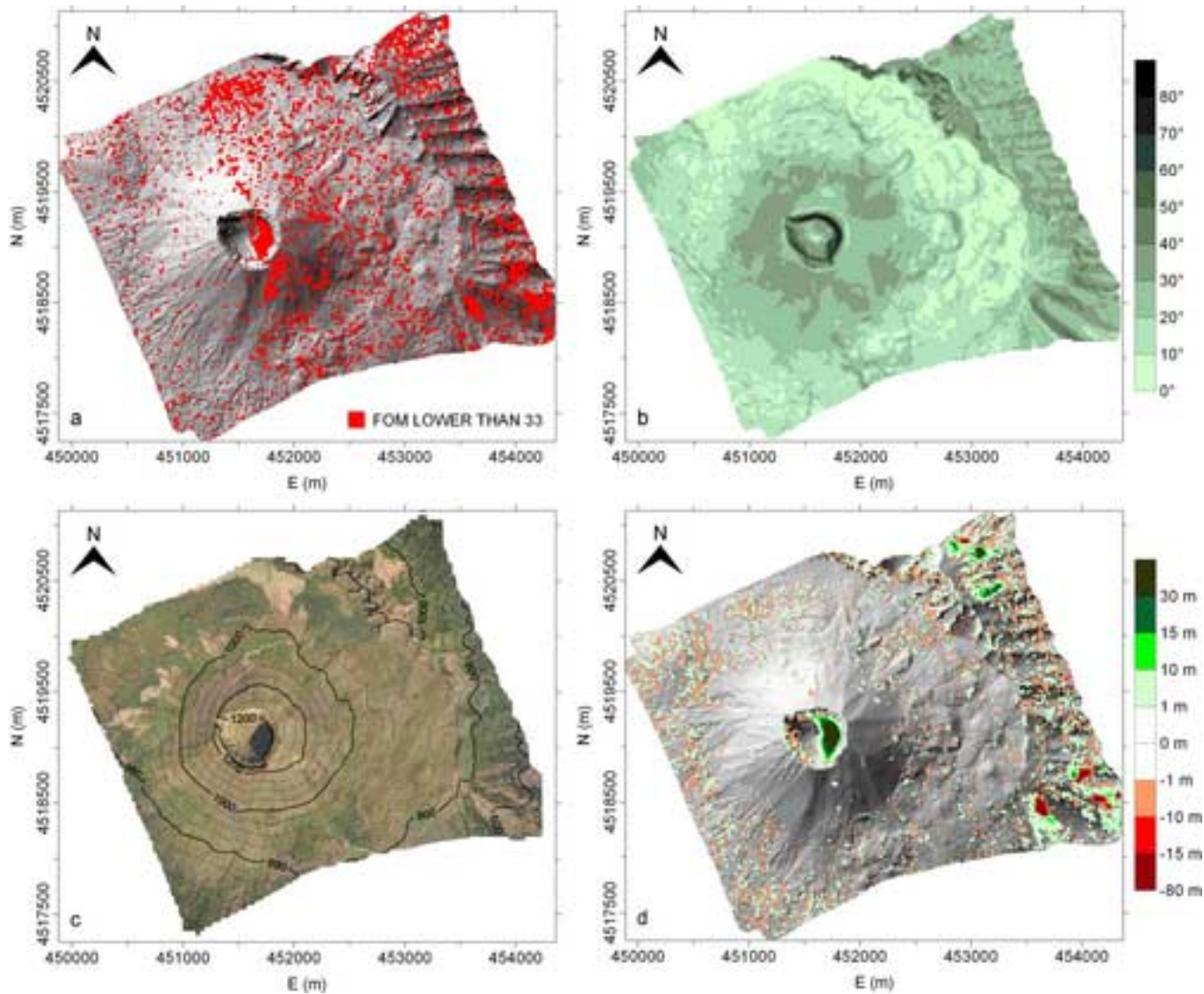


Figure4  
[Click here to download high resolution image](#)

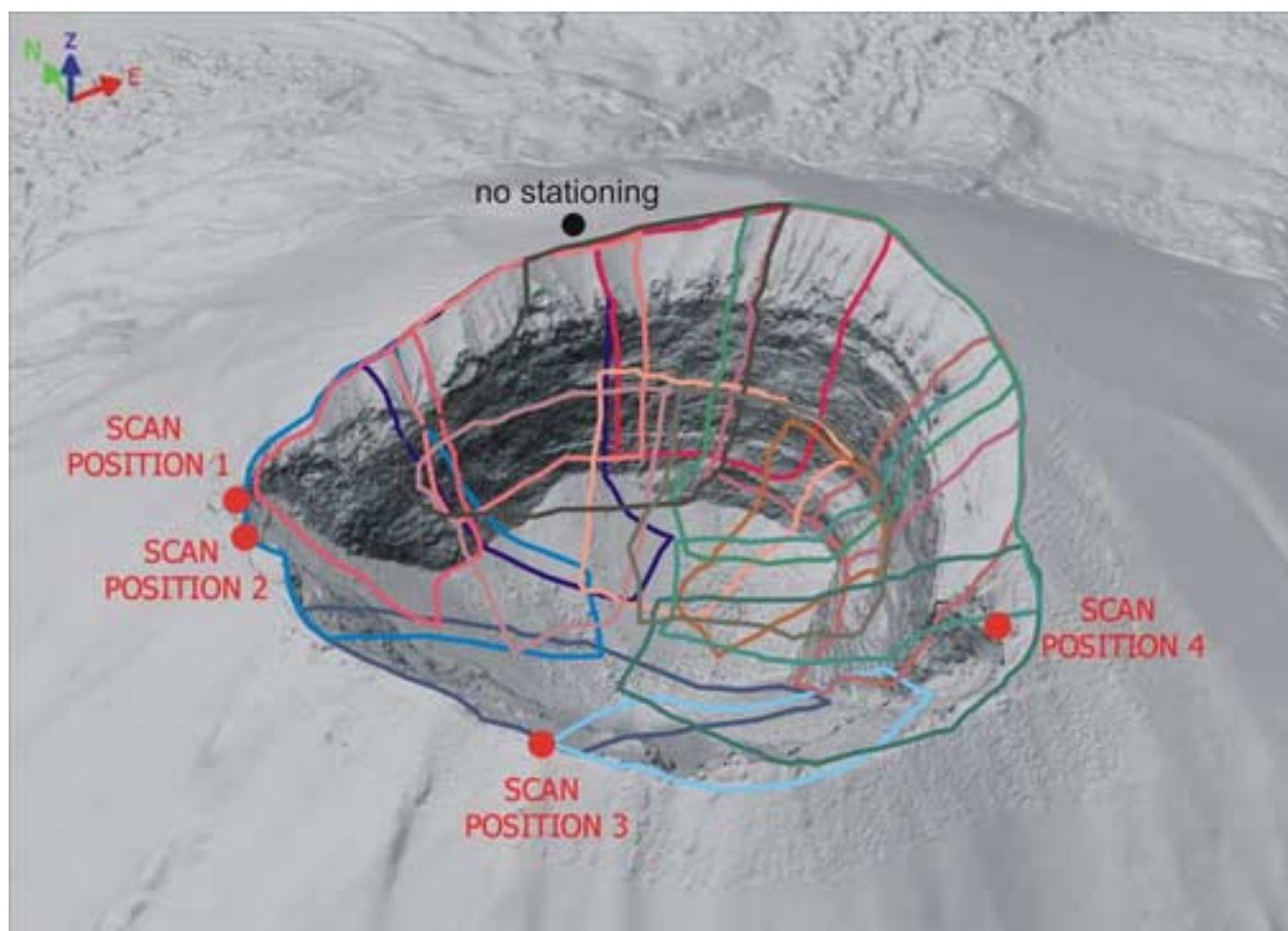




Figure5  
[Click here to download high resolution image](#)

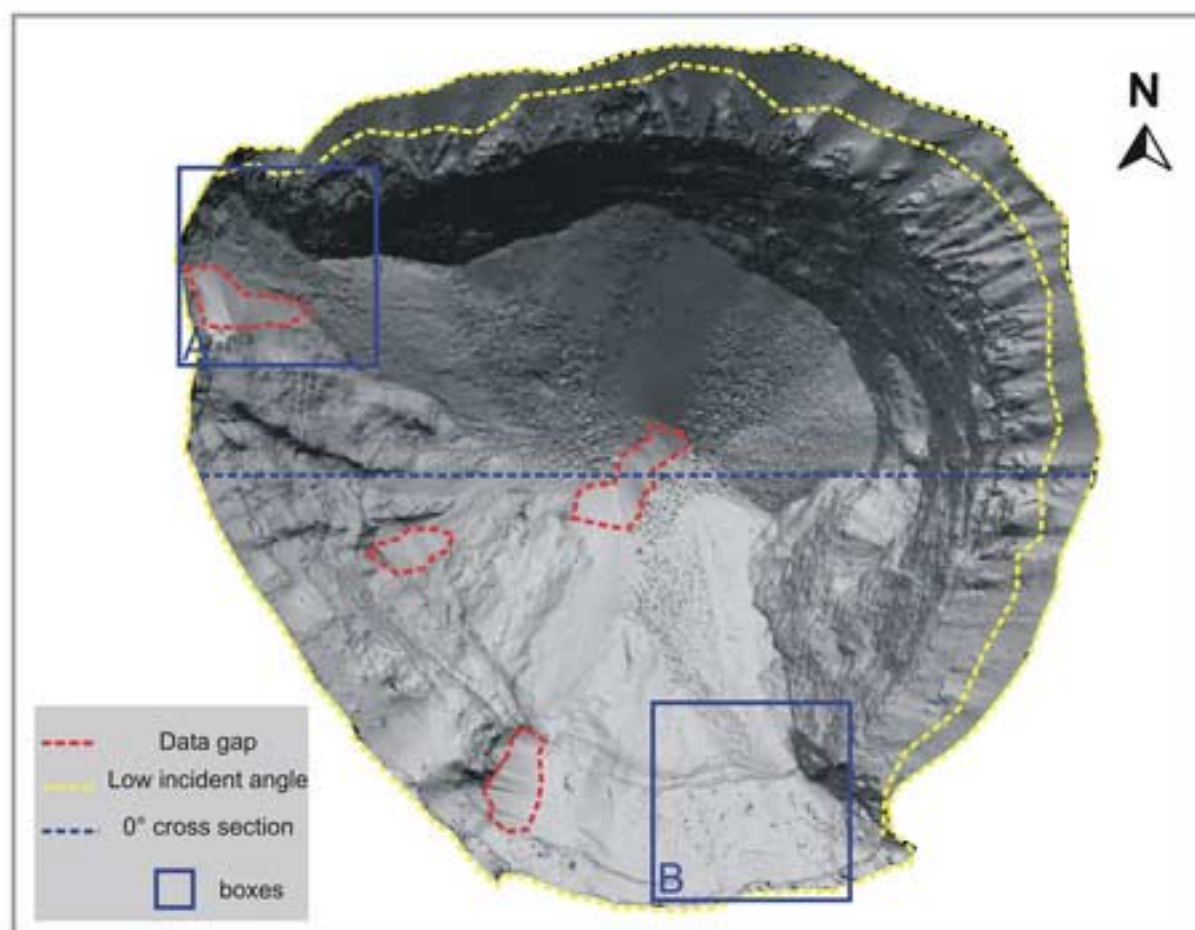


Figure6  
[Click here to download high resolution image](#)

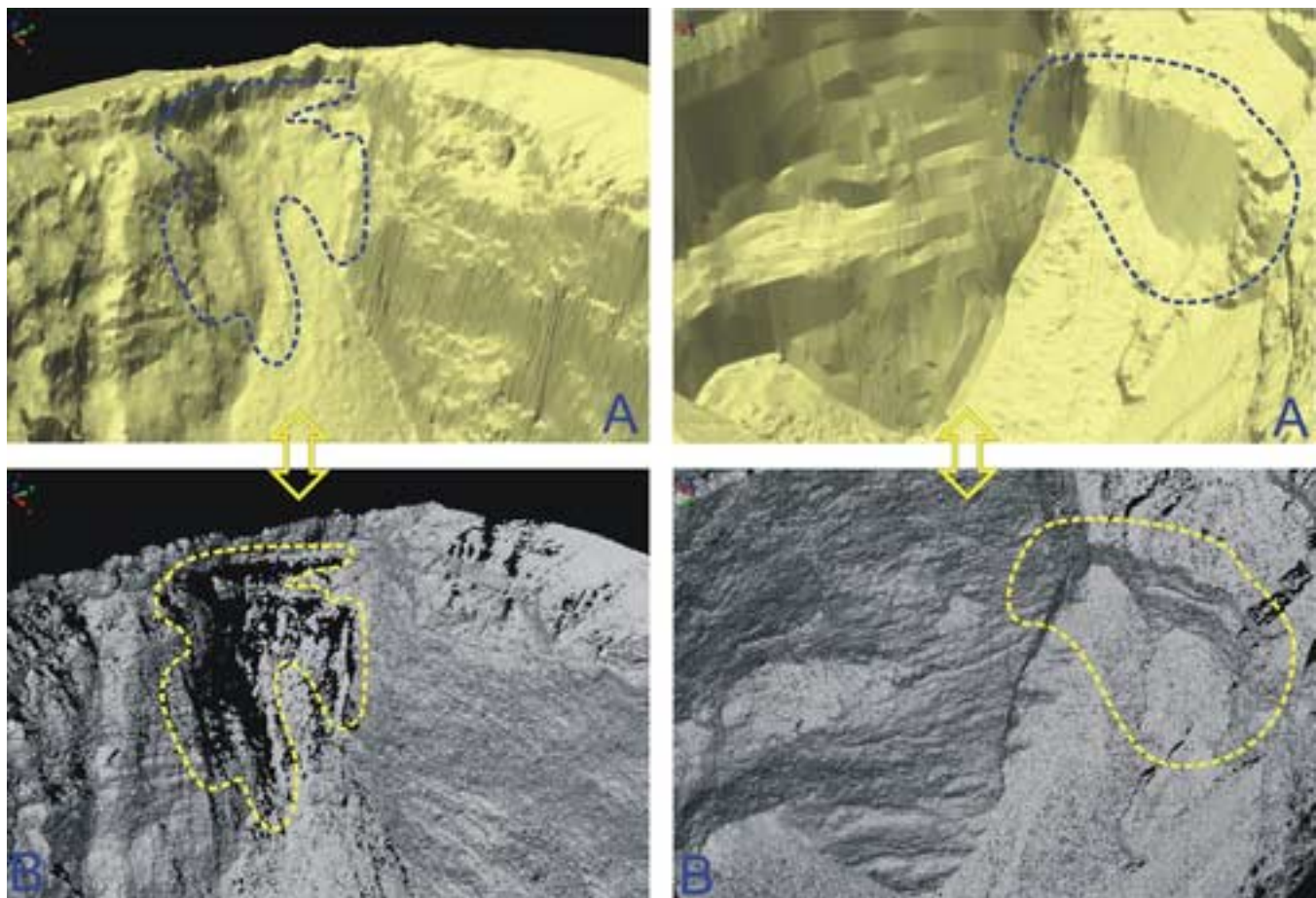


Figure7  
[Click here to download high resolution image](#)

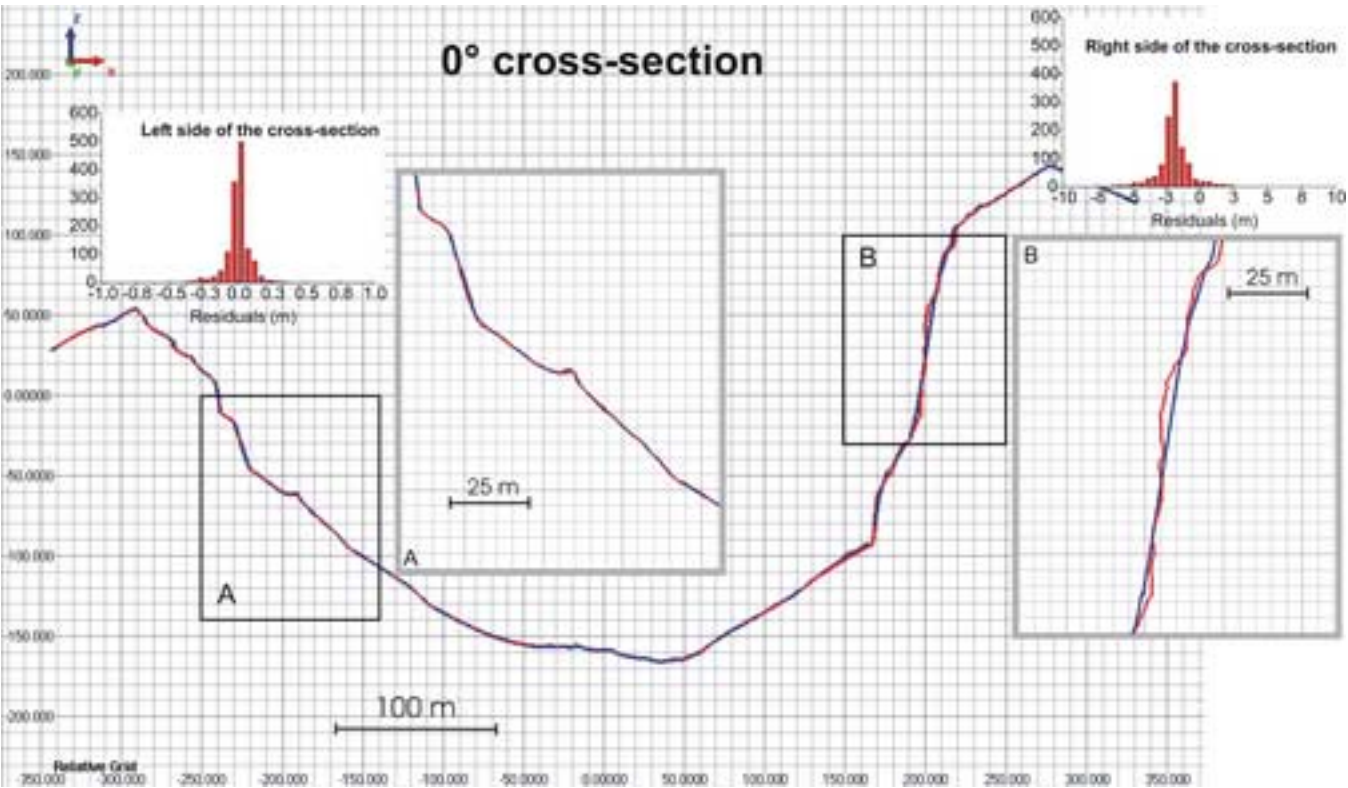


Figure8  
[Click here to download high resolution image](#)

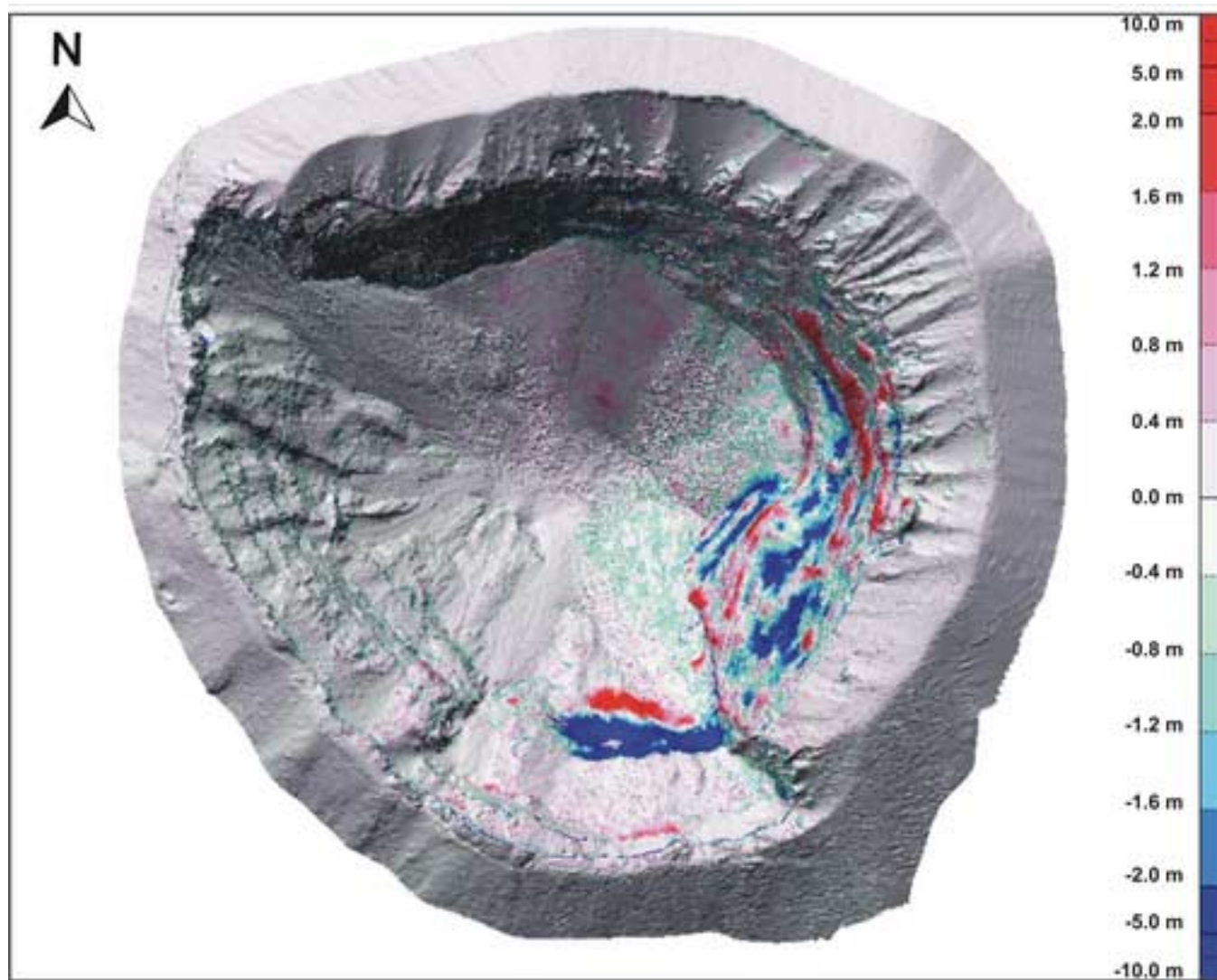




Figure9  
[Click here to download high resolution image](#)

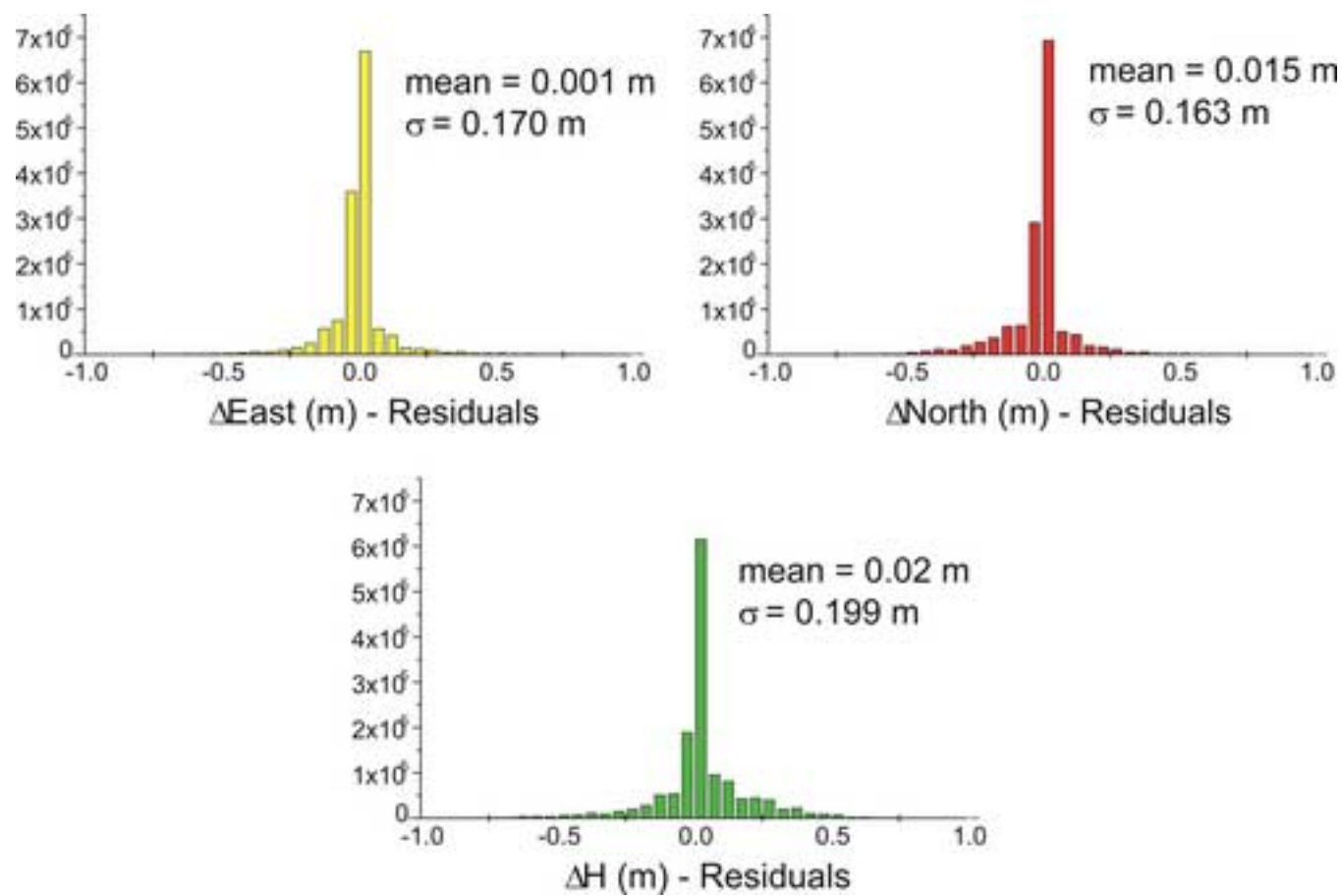


Figure10  
[Click here to download high resolution image](#)

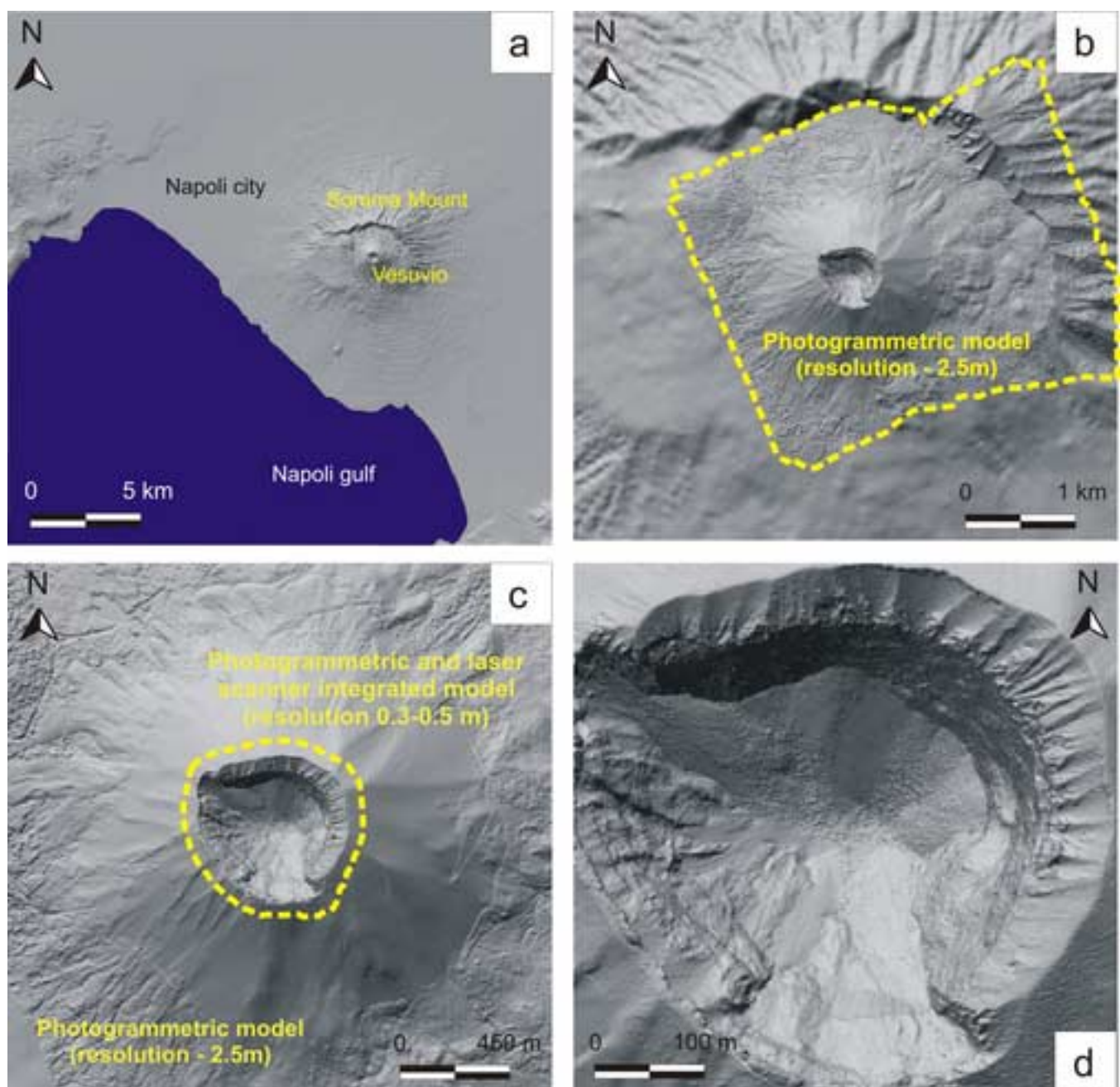


Figure11  
[Click here to download high resolution image](#)

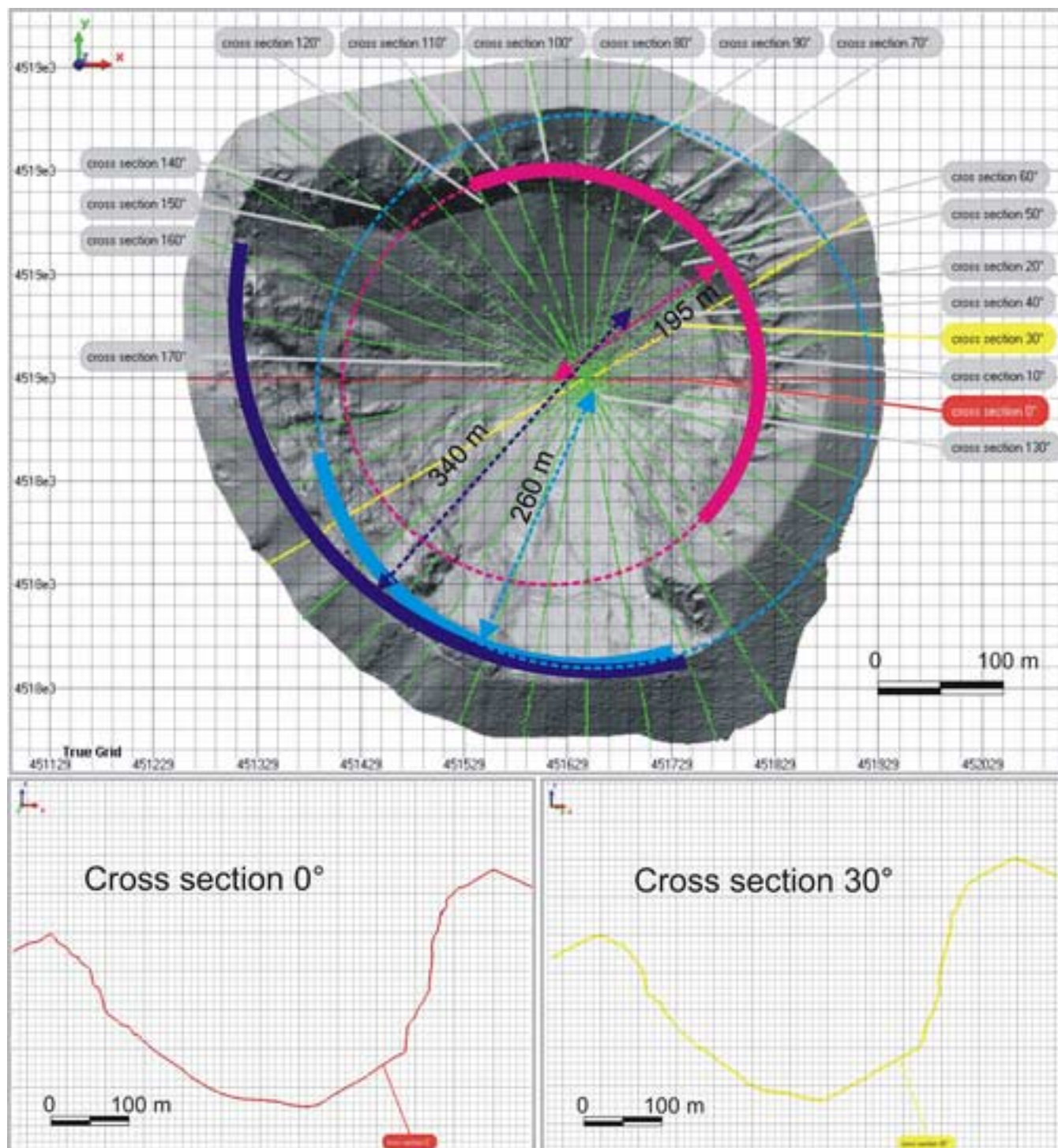




Figure12  
[Click here to download high resolution image](#)

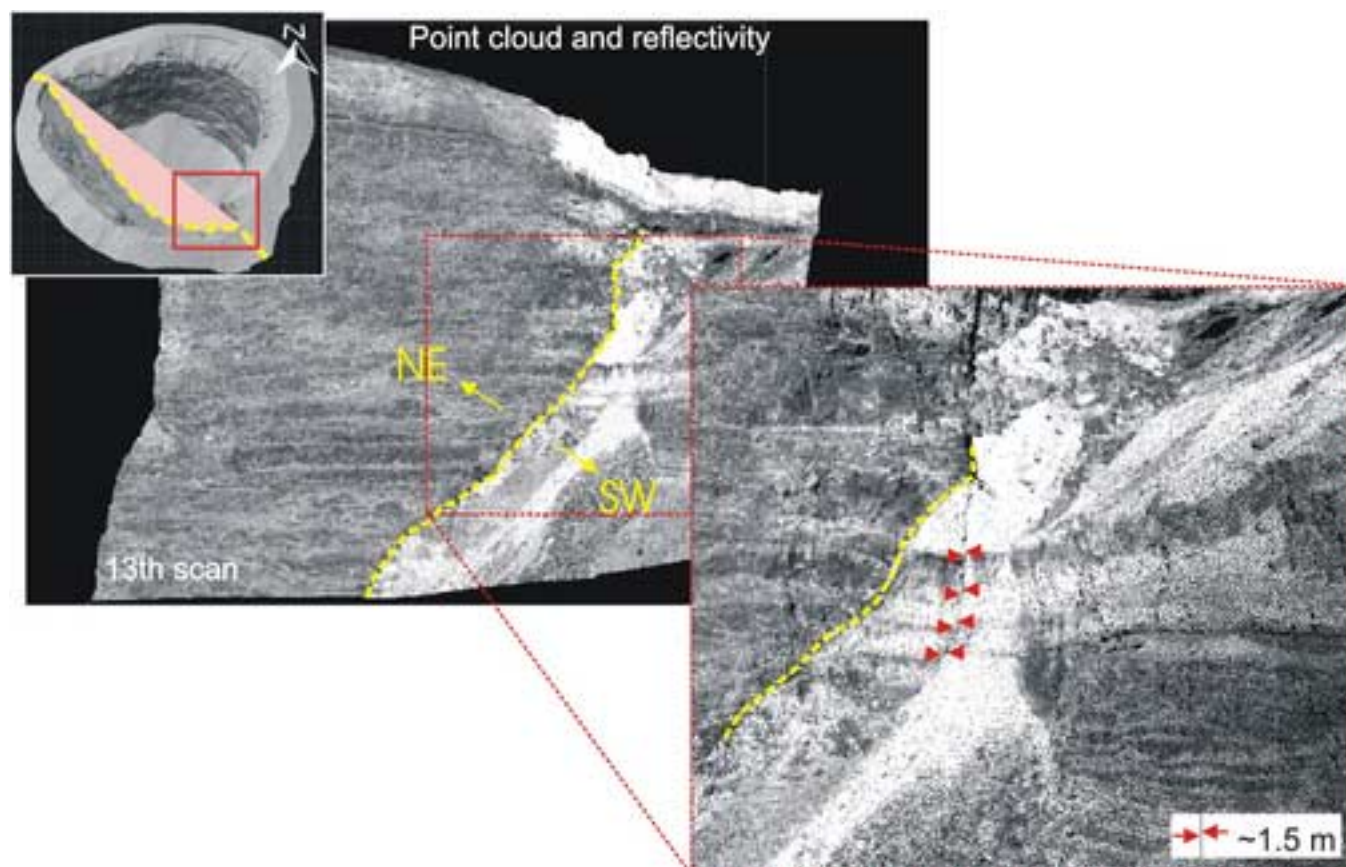




Figure13

[Click here to download high resolution image](#)

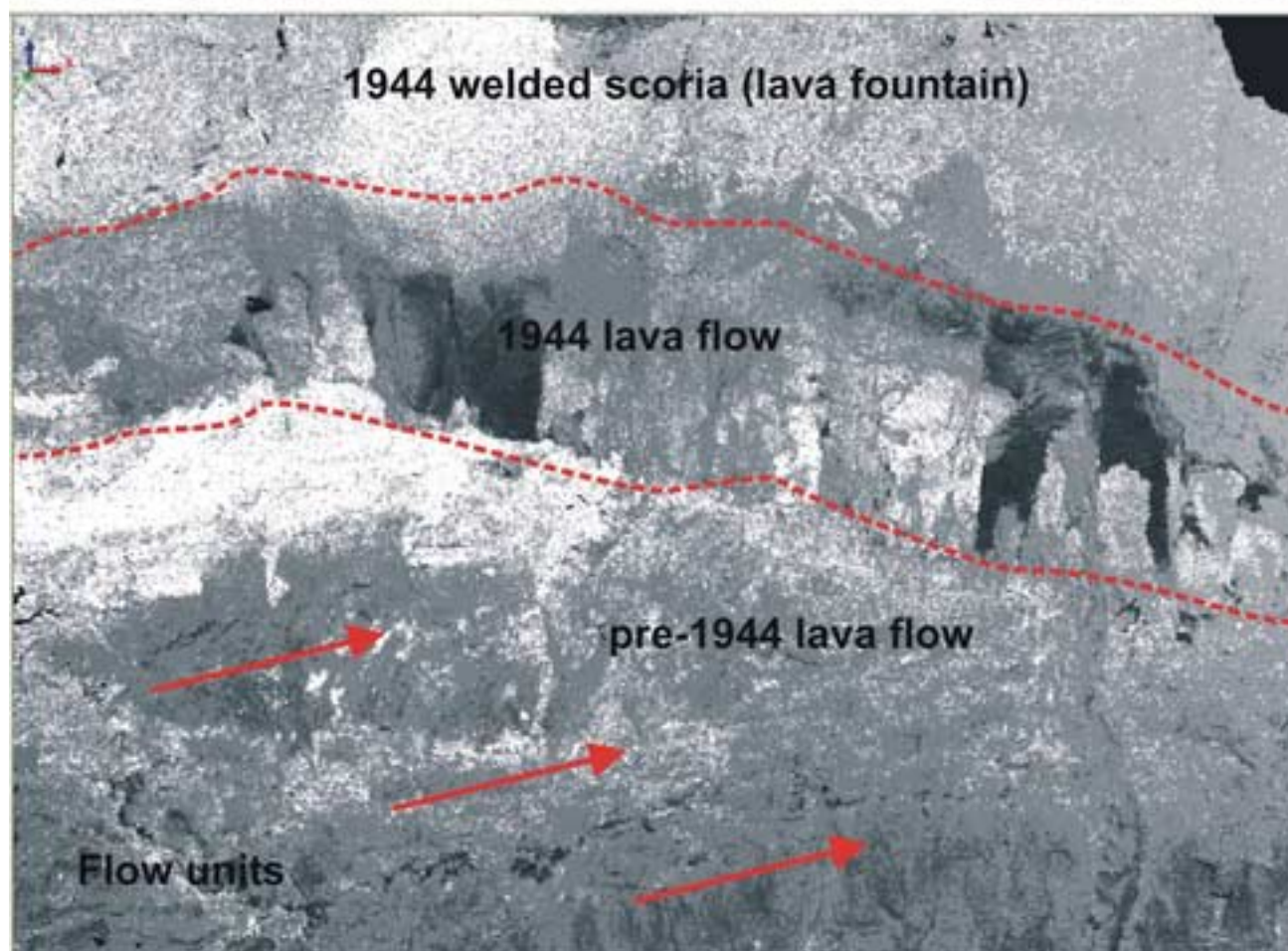
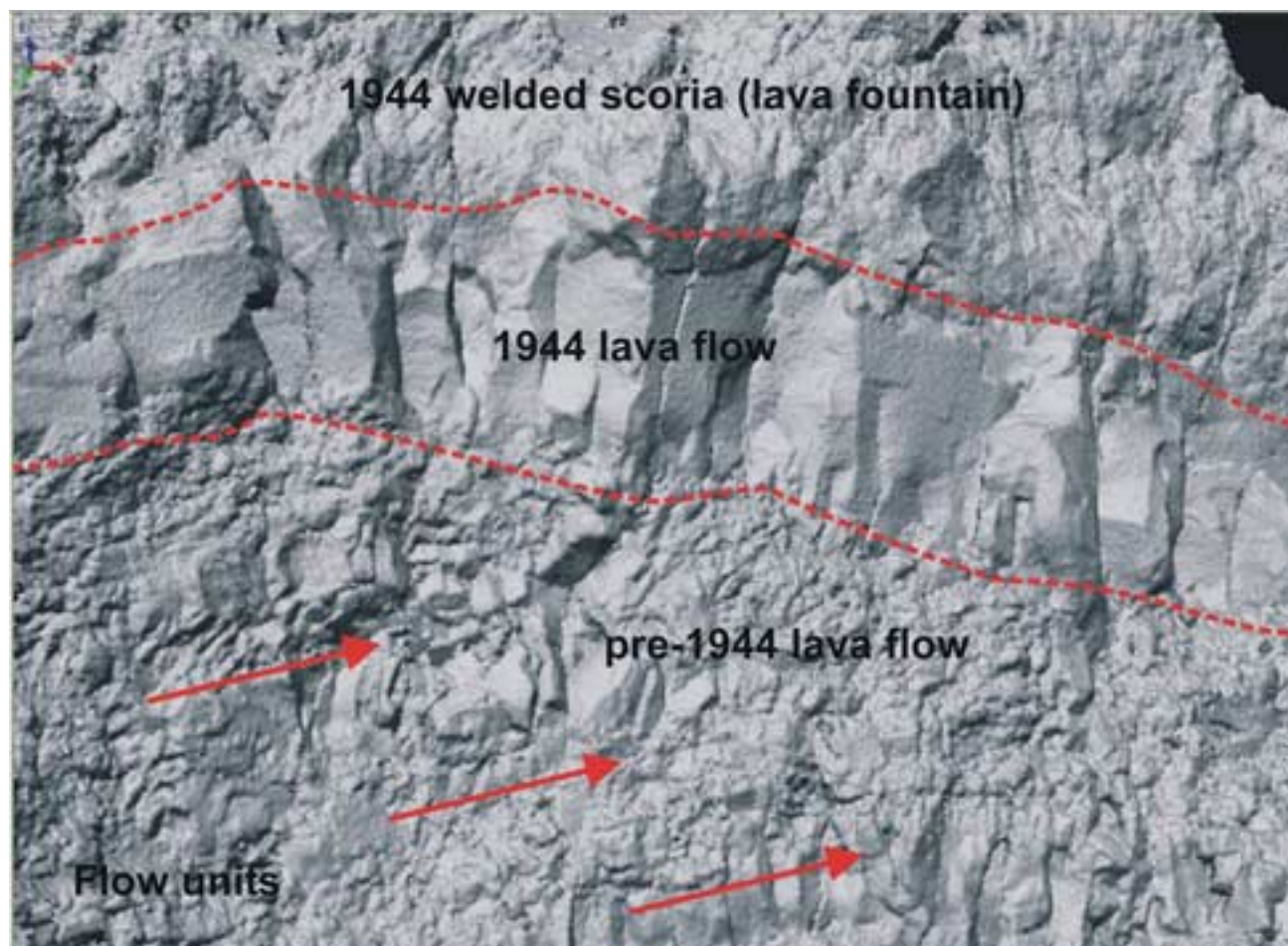
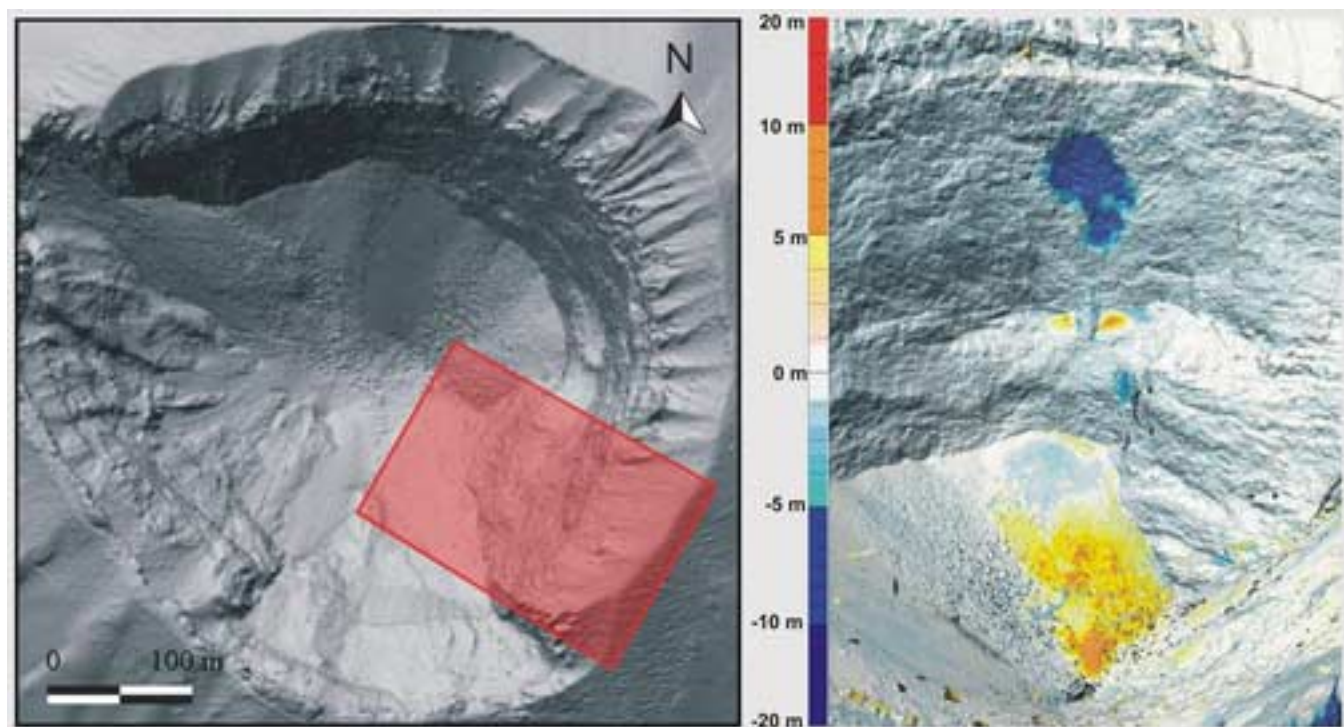


Figure14  
[Click here to download high resolution image](#)



Dear Margaret

we corrected carefully the references format.

figures were saved in JPG format at 300dpi (the tif format at 300 dpi provided too large size of files from 10MB to 40MB).

all the figures are considered in colour (web and paper) as indicated in the main text.

a further check of the english language was performed by our canadian colleagues.

thankyou very much.

Arianna Pesci & all the other authors..